Improvement in *a*-plane GaN crystalline quality using wet etching method*

Cao Rong-Tao(曹荣涛), Xu Sheng-Rui(许晟瑞), Zhang Jin-Cheng(张进成)†, Zhao Yi(赵 一), Xue Jun-Shuai(薛军帅), Ha Wei(哈 微), Zhang Shuai(张 帅), Cui Pei-Shui(崔培水), Wen Hui-Juan(温慧娟), and Chen Xing(陈 兴)

Key Laboratory of Wide Band-Gap Semiconductor Materials and Devices, School of Microelectronics, Xidian University, Xi'an 710071, *China*

(Received 4 May 2013; revised manuscript received 22 August 2013; published online 10 February 2014)

Nonpolar $(11\bar{2}0)$ GaN films are grown on the etched *a*-plane GaN substrates via metalorganic vapor phase epitaxy. High-resolution X-ray diffraction analysis shows great decreases in the full width at half maximum of the samples grown on etched substrates compared with those of the sample without etching, both on-axis and off-axis, indicating the reduced dislocation densities and improved crystalline quality of these samples. The spatial mapping of the E_2 (high) phonon mode demonstrates the smaller line width with a black background in the wing region, which testifies the reduced dislocation densities and enhanced crystalline quality of the epitaxial lateral overgrowth areas. Raman scattering spectra of the E_2 (high) peaks exhibit in-plane compressive stress for all the overgrowth samples, and the E_2 (high) peaks of samples grown on etched substrates shift toward the lower frequency range, indicating the relaxations of in-plane stress in these GaN films. Furthermore, room temperature photoluminescence measurement demonstrates a significant decrease in the yellow-band emission intensity of *a*-plane GaN grown on etched templates, which also illustrates the better optical properties of these samples.

Keywords: nonpolar GaN, wet etching, metal-organic chemical vapor deposition, crystalline quality

PACS: 78.55.Cr, 81.15.Kk **DOI:** 10.1088/1674-1056/23/4/047804

1. Introduction

Recently, GaN and nitride-based semiconductors have drawn extensive attention due to their potential applications in light emitting diodes ranging from the ultraviolet to the full visible of the electromagnetic spectrum.[1,2] With a *c*-plane sapphire or SiC substrate, the conventional *c*-plane GaN has an undesirable internal electric field deriving from the spontaneous and piezoelectric polarizations caused by the quantum-confined Stark effect.[3] The electric field existing, although advantageous for two-dimensional electron gas formation in transistors, leads to the spatial separation of electron and hole wave functions in the quantum well, reducing the luminescence efficiency and shifting the light emission toward the red wavelengths.[4] To solve these problems, the nitride-based devices and materials can be grown on the nonpolar GaN planes, such as the *a*- and *m*-planes.[5] The *c* axis lies within the nonpolar plane and provides no polarization field perpendicular to the layer interface. However, the high crystalline quality *a*- or *m*-plane GaN films with smooth surfaces are difficult to achieve due to high density stacking faults and threading dislocations.[6,7] In recent years, various methods have been employed to improve the quality of *a*-plane GaN such as traditional epitaxial lateral overgrowth (ELOG),[8–10] two-step growth process,[11] and application of TiN interlayer.[12] However, the traditional ELOG technique involves several photolithographic and etching steps in order to create a patterned template for the subsequent overgrowth process, which are costly, complex, and time consuming. The wet etching method, however, due to its low equipment cost, effective etching selection property, and minimal introduction of damage to the etched surfaces, has been widely used in the crystal quality improvement of conventional *c*-plane GaN in recent years.[13–16] However, detailed reports and systematic investigations of the overgrowth GaN on etched *a*-plane GaN substrates are lacking.

In the following, we present a detailed research of the *a*-plane GaN grown on the etched nonpolar GaN template using the wet etching method. We analyze the changes of crystal quality and stress using different experimental methods such as high-resolution X-ray diffraction (HRXRD), photoluminescence (PL), Raman spectroscopy, and spatial mapping of the E_2 (high) phonon mode.

2. Experimental procedure

Three *a*-plane GaN film samples each with a thickness of 3 μm were grown on *r*-plane $(1\bar{1}02)$ sapphire substrates at 1000 °C in a cold-wall showerhead metal–organic chemical vapor deposition (MOCVD) system. A low-temperature

*Project supported by the National Natural Science Foundation of China (Grant No. 61204006), the Fundamental Research Funds for the Central Universities, China (Grant No. K50511250002), and the National Key Science & Technology Special Project, China (Grant No. 2008ZX01002-002).

†Corresponding author. E-mail: jchzhang@xidian.edu.cn

© 2014 Chinese Physical Society and IOP Publishing Ltd

AlN (LT-AlN) nucleation layer 25 nm in thickness and a high-temperature AlN (HT-AlN) layer 100 nm in thickness were grown at 615 °C and 1075 °C, respectively. These three GaN films were then used as templates for the subsequent wet etching process. One of these samples was used as the reference substance called sample A. Samples B and C were etched in H_3PO_4 with a concentration of over 97% at 130 °C for 5 min and 8 min, respectively. After chemical cleaning, all these samples were loaded in the same MOCVD chamber. Prior to the epitaxial growth, all the samples were annealed at 1050 °C in the NH_3 atmosphere for 10 min to remove the surface contaminations. Then 6-μm thick GaN film was grown on each substrate at 1045 °C and 5.3×10^3 Pa. Trimethylgallium, trimethylaluminium, and ammonia (NH_3) were used as sources of Ga, Al, N, respectively. Hydrogen was used as the carrier gas in this experiment.

The morphology of etched *a*-plane GaN was investigated by scanning electron microscopy (SEM). HRXRD measurement was realized using a Bruker D8-discover system equipped with a Ge (220) monochromator and channel-cut analyzer operating in triple-axis mode, delivering a pure Cu K_α line of wavelength $\lambda = 0.15406$ nm. A 514-nm argon laser was performed to demonstrate the Raman spectrum and spatial mapping of the E_2 (high) phonon mode. The PL spectrum was also measured using the 325-nm line of an He–Cd laser.

3. Results and discussion

Figure 1 shows the surface morphology of the etched *a*-plane GaN with hot H_3PO_4 for 8 min at 130 °C. The etching direction is along the $-c$ axis [000$\bar{1}$], for the (000$\bar{1}$) plane existing in the basal plane stacking faults (BSF) of the triangular pits is N-face, and along the direction the etching speed is fast compared with that along other directions, such as the $+c$ axis [0001].[17] Thus, the selective etching process creates channels along the $-c$ direction on the surface, which serves as the patterned structure for the subsequent overgrowth process.

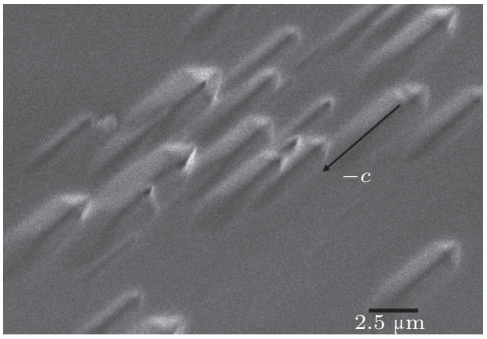


Fig. 1. SEM image of etched *a*-plane GaN.

Figure 2 shows the 2θ–ω X-ray diffraction scan of sample C in a range from 52° to 58.3°. Two peaks exist in this range: (2$\bar{2}$04) *r*-sapphire at 52.7° and (11$\bar{2}$0) *a*-plane GaN at 57.6° different from the *c*-plane GaN at 34.6°. The results in Fig. 1 demonstrate experimentally that the overgrowth GaN film is nonpolar GaN. The growing *a*-plane GaN on *r*-sapphire can be explained theoretically by the previous analysis of Sano and Aoki,[18] and Sasaki and Zembutsu.[19]

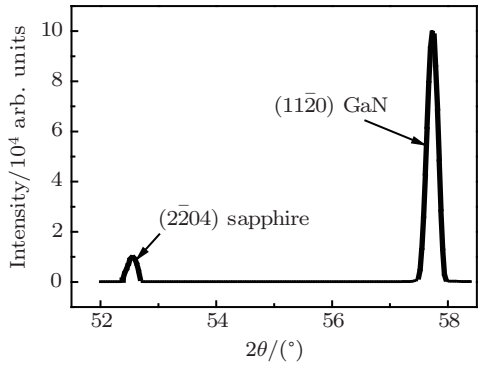


Fig. 2. 2θ–ω scan of sample C.

As is well known, the full widths at half maximum (FWHM) of the omega-scan rocking curve for symmetric and skew symmetric planes indirectly indicate the densities of screw and edge dislocations with the mean tilt and twist angles of mosaic crystals, respectively. Moreover due to the anisotropic mosaic broadening, a single omega X-ray rocking curve (XRC) cannot estimate the quality of GaN grown on *r*-plane sapphire. Thus the two XRC scans of *a*-plane GaN along the *c* and *m* axes are performed for the proper judgment of the crystalline quality. We also measure the skew symmetric planes (10$\bar{1}$1) XRC. The results are listed in Table 1.

Table 1. Results of on-axis (11$\bar{2}$0) and off-axis (10$\bar{1}$1) FWHMs of samples A, B, and C.

Sample	*c*-axis XRC FWHM/arcsec	*m*-axis XRC FWHM/arcsec	10$\bar{1}$1 XRC FWHM/arcsec
A	717	1169	1997
B	625	1094	1981
C	678	1143	2008

According to Table 1, the *c*-axis FWHMs of samples B and C with the incident X-ray beam parallel to the [0001] direction are 625 arcsec and 678 arcsec, which are nearly 13% and 6% lower than the value 717 arcsec of sample A, respectively. The *m*-axis FWHMs of samples B and C with the incident X-ray beam parallel to the [1$\bar{1}$00] direction are 1094 arcsec and 1143 arcsec, which are also lower than the value 1169 arcsec of sample A. Also, the (10$\bar{1}$1) XRC FWHM of sample B is 1981 arcsec, lower than the value 1997 arcsec of sample A. However, the (10$\bar{1}$1) XRC FWHM of sample C, with a value of 2008 arcsec, is slightly higher than that

of sample A. Moreover, we also find that there are considerable differences in the FWHM value among the c, m axes, and the $(10\bar{1}1)$ planes for each sample; this phenomenon can be attributed to the anisotropy in different directions for the a-plane GaN.[20] Compared with sample B, sample C has high FWHMs along the a, c axes and the $(10\bar{1}1)$ plane, representing the deteriorative crystal quality. This phenomenon can be explained by the over etched substrate of sample C for 8 min, which creates too large pits and leads to the difficulty in coalescing the subsequent a-plane GaN overgrowth process. The overgrowth processes of the etched a-plane GaN substrates of samples B and C can be explained by Fig. 3.

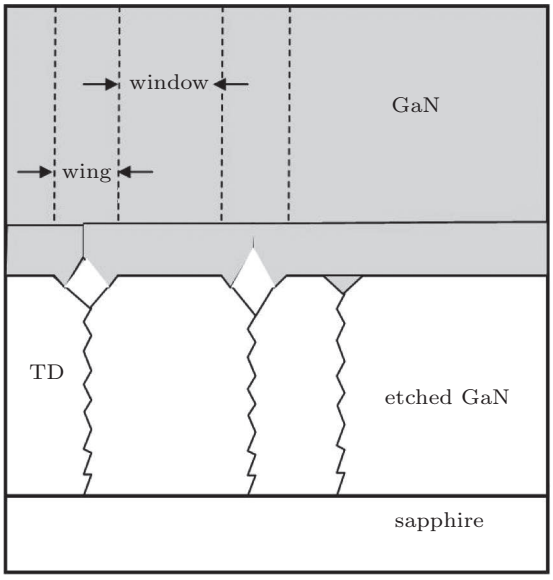


Fig. 3. Schematic diagram of overgrowth process on etched a-plane GaN substrate.

As can be seen in Fig. 3, the etching method used in samples B and C create pits with different sizes in the GaN substrates, which serve as patterned structures for the later overgrowth process. The wing regions tend to be coalesced at the top of the etched pits, resulting in the reduction of dislocations and the improvement in crystal quality in these regions. This process, known as ELOG,[21] provides the defect selective passivation rather than the random blocking of dislocations, which helps to explain the significant decrease in FWHM along the c axis of sample B, for the etching and coalescent processes are along the $-c$ axis and the m axis, respectively. However, larger pits created by the etching process, with a longer time for the substrate of sample C, would need a longer time to be coalesced. The growth time and condition in this experiment are not enough for sample C to be completely coalesced, thereby resulting in the deterioration in the crystal quality. What is more, the limited improvement in crystal quality with this method can be partially explained by the small areas of epitaxial regions. An epitaxial region is the region where the dislocations collide and disappear, leaving the region with a higher crystal quality and a lower dislocation density. However, with the etching process along the $-c$ direction of the region with BSFs and the limited BSF density on the surface of the sample, the etching process creates limited channels severing as epitaxial regions for the subsequent overgrowth, indicating the incomplete reduction of dislocations and the limited crystal quality improvement. However, compared with the crystal quantities obtained using other methods such as the conventional ELOG method,[22] the crystal quality obtained using the present method is quite dramatically improved. More detailed explanations and analysis of the limited crystal quality enhancement will be investigated in the future.

Raman scattering is widely used to investigate hexagonal wurtzite GaN film grown on a sapphire substrate, owning to its nondestructive and contactless features. The E_2 (high) phonon mode is sensitive to the stress and can provide useful quality information about the GaN structure. Thus, a spatial mapping of the E_2 (high) phonon mode is adopted as an effective way to measure the change of the GaN crystalline quality in the ELOG region. Figure 4 shows the E_2 (high) phonon line width change in the overgrowth sample after the etching process with a selected area of about 10 μm × 10 μm. The contrast in line width between the wing and window regions is apparent. The black background regions with lower line width of E_2 (high) phonon mode indicate the crystalline quality improvement in the wing regions, which testifies the existence of the effect of reducing dislocations through ELOG after the wet etching process on the substrates by hot H_3PO_4.

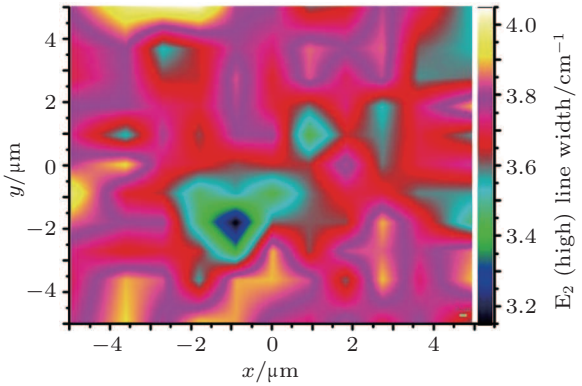


Fig. 4. (color online) Raman mapping image of E_2 (high) phonon line width of the overgrowth sample.

Normalized Raman scattering spectra of E_2 (high) peaks in samples A, B, and C are analyzed at room temperature to determine the stress states of the overgrowth samples on the

etched *a*-plane GaN substrates. The backscattering configuration $x(yy)$–x is adopted, where x and y denote the $[11\bar{2}0]$ and $[1\bar{1}00]$ directions of the *a*-plane GaN, respectively. A_1 (TO) and E_2 (high) peaks are the allowed modes under this configuration,[23] as can be clearly observed in Fig. 5.

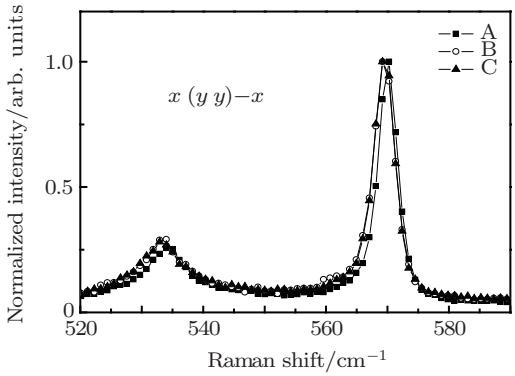


Fig. 5. Raman spectra obtained through backscattering configuration $x(yy)$–x of samples A, B, and C.

The residual in-plane strain in wurtzite GaN can be measured by evaluating the shift value of the frequency of the E_2 (high) mode. The E_2 (high) frequencies of samples A, B, and C are 570.1, 569.4, and 569.3 cm^{-1}, respectively. With respect to the strain-free GaN of 568 cm^{-1} and a value of 2.7 cm^{-1}/GPa serving as a linear proportionality factor between the shift in the E_2 (high) phonon mode and stress, we determine the compressive stresses of 0.78 GPa, 0.52 GPa, and 0.48 GPa from the shifts of E_2 (high) modes to have 2.1 cm^{-1}, 1.4 cm^{-1}, and 1.3 cm^{-1} deviating from the reference frequency, which indicates a large compressive strain for each of all the samples. Moreover, samples B and C shift to the lower frequency toward the free strain state than sample A, representing the in-plane strain release of the overgrowth *a*-plane GaN after the etching process. The relaxation of the stress should be associated with the lower density of dislocations after the ELOG process.

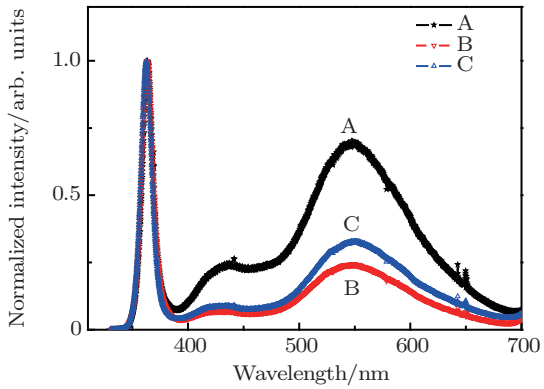


Fig. 6. (color online) PL spectra of samples A, B, and C.

In order to determine the luminescence influence of the etching process on *a*-plane GaN overgrowth, the PL measurement is performed at room temperature. Figure 6 shows the normalized PL spectra to the near band emission of these three samples. Compared with sample A, samples B and C each have a much lower yellow luminescence (YL) emission intensity. At the same time, sample C shows an apparently higher YL emission intensity than sample B. The origin of the well-known YL band centered at 550 nm in the luminescence spectrum of GaN is associated with the impurities and complexes.[24,25] The dislocations, mainly the partial dislocation associated with BSFs in *a*-plane GaN, serve as the non-radioactive recombination centers and limit the efficiency of radioactive recombination. Thus, the lower intensities of YL emission of samples B and C indicate the reduced dislocations and enhanced overgrowth crystal quality on etched substrates.

4. Conclusions

In this paper, we created the patterned substrates in *a*-plane GaN by the wet etching method with hot H_3PO_4 for the subsequent overgrowth process, and the *a*-plane overgrowth GaN with the significant improved crystalline quality was achieved. The sample B under an appropriate etching condition shows a considerable decrease in FWHM as a result of the reduced dislocations and BSF density. The hues of the spatial mapping of the E_2 (high) phonon mode ranging from black for the background to red, are measured to illustrate the quality improvement in ELOG regions on patterned substrates. In the Raman spectrum, the E_2 (high) peaks of sample B and C shifting to the lower frequencies demonstrate the release of compressive stress in the etched *a*-plane GaN overgrowth samples. From the results of PL normalized spectra, we also find that samples B and C have the low intensities of yellow luminescence compared with sample A, indicating the reduced dislocation density and enhanced overgrowth GaN quality on an etched substrate with hot H_3PO_4.

References

[1] Xu S R, Hao Y, Zhang J C, Xue X Y, Li P X, Li J T, Lin Z Y, Liu Z Y, Ma J C, He Q and Lü L 2011 *Chin. Phys. B* **20** 107802
[2] Zhang J F, Xu S R, Zhang J C and Hao Y 2011 *Chin. Phys. B* **20** 057801
[3] Bernardini F, Fiorentini V and Vanderbilt D 1997 *Phys. Rev. B* **56** R10024
[4] Cho Y S, Sun Q, Lee I H, Ko T S, Yerino C D, Han J, Kong B H, Cho H K and Wang S 2008 *Appl. Phys. Lett.* **93** 111904
[5] Waltereit P, Brandt O, Trampert A, Grahn H T, Yang J W and Khan M A 2000 *Nature* **406** 865
[6] Liu R, Bell A, Ponce F A, Chen C Q, Yang J W and Khan M A 2005 *Appl. Phys. Lett.* **86** 021908
[7] Wu Z H, Fischer A M, Ponce F A, Bastek B, Christen J, Wernicke T, Weyers M and Kneissl M 2008 *Appl. Phys. Lett.* **92** 171904
[8] Craven M D, Lim S H, Wu F, Speck J S and DenBaars S P 2002 *Appl. Phys. Lett.* **81** 1201
[9] Haskell B A, Wu F, Craven M D, Matsuda S and Fini P T 2003 *Appl. Phys. Lett.* **83** 644
[10] Johnston C F, Kappers M J, Moram M A, Hollander J L and Humphreys C L 2009 *J. Cryst. Growth* **311** 3295

[11] Hollander J L, Kappers M J, McAleese C and Humphreys C 2008 *Appl. Phys. Lett.* **92** 101104
[12] Xu S R, Zhang J C, Yang L A, Zhou X W, Cao Y R, Zhang J F, Xue J S, Liu Z Y, Ma J C, Bao F and Hao Y 2011 *J. Cryst. Growth* **327** 94
[13] Stocker D A, Schubert E F and Redwing J M 1998 *Appl. Phys. Lett.* **73** 2654
[14] Na S I, Ha G Y, Han D S, Kim S S, Kim J Y, Lim J H, Kim D J, Min K I and Park S J 2006 *IEEE. Photon. Technol. Lett.* **18** 14
[15] Youtsey C, Adesida I, Romano L T and Bulman G 1998 *Appl. Phys. Lett.* **72** 560
[16] Youtsey C, Romano L T and Adesida I 1998 *Appl. Phys. Lett.* **73** 797
[17] Rouviere J L, Weyher J L, Seelmann-Eggbert M and Porowski S 1998 *Appl. Phys. Lett.* **73** 668
[18] M. Sano and M. Aoki 1976 *Jpn. J. Appl. Phys.* **15** 1943
[19] T. Sasaki and S. Zembutsu 1987 *J. Appl. Phys.* **61** 2533
[20] Xu S R, Hao Y, Zhang J C, Zhou X W, Yang L A, Zhang J F, Duan H T, Li Z M, Wei M, Hu S G, Cao Y R, Zhu Q W, Xu Z H and Gu W P 2009 *J. Cryst. Growth* **311** 3622
[21] Mukai T, Takekawa K and Nakamura S 1998 *Jpn. J. Appl. Phys., Part 2* **37** L839
[22] Chakraborty A, Kim K C, Wu F, Speck J S, Denbaars S P and Mishr U K 2006 *Appl. Phys. Lett.* **89** 041903
[23] Yan F W, Gao H Y, Zhang H X, Wang G H, Zeng Y P, Yan J C, Wang J X, Zeng Y P and Li J M 2007 *J. Appl. Phys.* **101** 023506
[24] Mickevi‘eius J, Aleksiejunas R, Shur M S, Sakalauskas S, Tamulaitis G, Fareed Q and Gaska R 2005 *Appl. Phys. Lett.* **86** 041910
[25] Neugebauera J and Walle C V 1996 *Appl. Phys. Lett.* **69** 503